Chemistry of Molecular Growth Processes in Flames

Kermit C. Smyth and J. Houston Miller

Chemical mechanisms of pyrolysis, growth, and oxidation processes in flames have traditionally been inferred from spatial profile measurements of species concentrations. Experimental investigations now include the detection of numerous minor species such as reactive radicals and intermediate hydrocarbons. In assessing a proposed mechanism important new constraints can be established when the detailed species profile data are combined with velocity and temperature measurements and analyzed to determine production and destruction rates for specific molecules. Recent results on hydrocarbon diffusion flames provide new information on the interplay between chemical and transport processes. These measurements have led to direct tests of proposed routes for the formation of aromatic hydrocarbons and the first, small soot particles. The inception chemistry of hydrocarbon growth reactions and initial particle formation is thought to control soot formation, flame radiation and energy transfer, and pollutant emission in combustion environments.

CHEMICAL GROWTH AND OXIDATION ARE IMPORTANT PROcesses that occur at elevated flame temperatures. The steps by which hydrocarbon molecules are transformed into larger species are especially interesting since these reactions lead to dramatic consequences in many combustion environments. For example, the formation of intermediate hydrocarbons, such as polycyclic aromatic hydrocarbons (PAHs), occurs under fuel-rich conditions and poses a potential long-term health hazard because many PAHs are carcinogenic. These compounds are also involved in further growth reactions that lead to the formation of soot particles. Radiation from soot dominates the energy transfer from large fires, and thus soot formation plays a key role for combustion efficiency in furnaces and for flame spread in fires. Particle formation and radiative energy transfer also control the amount of smoke produced, which is important in fire detection, visual obscuration that hinders escape from a fire, and pollutant emission. The identification of the detailed formation mechanisms of large hydrocarbons produced during combustion continues to be one of the most challenging problems in high-temperature chemistry. After many decades of speculation, recent experimental and modeling efforts have yielded significant advances in our understanding of the important steps in hydrocarbon growth chemistry as well as of the key role of acetylene in subsequent particle growth.

Soot formation in a hydrocarbon flame involves a series of distinct steps that include (i) the production of precursor molecules, which react rapidly to give larger species; (ii) chemical growth that results in the formation of numerous small primary particles (diameter ≥ 2 nm); (iii) particle growth by surface reactions as well as by coagulation and agglomeration; and (iv) competing particle oxidation. Despite the fact that almost all of the soot mass is provided by surface growth reactions, it is now believed that particle inception (steps i and ii) controls the amount of soot ultimately produced (*1–5*). This situation arises because the earliest chemical steps are the critical bottlenecks and are thus rate-limiting: fuel pyrolysis chemistry (step i) (*1*) and the formation of the initial surface area available for particle growth (step ii) (*2–4*) are both important. Investigations of soot formation have shown that the soot concentrations, the soot radiation, the temperature field, and the final smoke emission from a hydrocarbon flame are all closely linked to the initial steps of particle inception (*5*).

Although the importance of the mechanisms for precursor formation and chemical growth processes has been well recognized, quantitative measurements on these key steps have been limited. Several models for the chemical mechanism of hydrocarbon molecular growth have been advanced which postulate that ions (*6*), PAHs (*7*), polyacetylenic chains (*8*), or neutral radicals (*9*) are the most significant intermediates. However, stringent tests of these proposed mechanisms can only be made with species profile data obtained in flames. Furthermore, since the chemical and transport processes are closely coupled, the determination of species production and destruction rates provides additional constraints on chemical growth models. Numerous measurements of the chemical composition have been made in premixed flames (*7, 8, 10–15*) in which the fuel and oxidizer are mixed together at a known composition prior to burning. A significant advance has recently been achieved by Howard and co-workers (*11, 13*), who have combined extensive profile results with temperature and flow field data to calculate how rapidly intermediate hydrocarbons are produced and destroyed. These species concentration data and the time-temperature history in one-dimensional (flat), premixed flames have been used to both generate and test models for molecular growth (*11, 13, 16*).

For studies of chemical growth processes in diffusion flames, where the fuel and oxidizer are introduced separately, new insight is provided when the time rate of change of hydrocarbon concentrations can be determined through the combination of concentration, temperature, and velocity measurements. In this regard the analysis of data obtained in premixed flames by Howard and co-workers has been the foundation and guiding example for recent work in hydrocarbon diffusion flames. Although many earlier sampling studies have also been performed on diffusion flames (*17*), only recently have detailed concentration measurements for a number of hydrocarbon molecules been reported (*18–21*). These new diffusion

---

K. C. Smyth is at the Center for Fire Research, National Bureau of Standards, Gaithersburg, MD 20899. J. H. Miller is at the Department of Chemistry, George Washington University, Washington, DC 20052.

flame results are significant since we can now test our understanding of chemical growth processes in flame systems that more closely resemble many practical combustion environments. In addition, it is important to compare the fastest routes for the production of intermediate hydrocarbons as determined from the analysis of premixed and diffusion flame measurements. Is there a universal mechanism for soot formation?

This article describes recent research that has improved our understanding of the early chemical steps of molecular growth in hydrocarbon flames. In particular, detailed results on a simple methane/air diffusion flame are discussed and compared with studies on premixed flames and with models that are used in the analysis of several high-temperature systems (heated flow tubes, very low pressure pyrolysis cells, shock tubes, and premixed flames). For the diffusion flame investigations three steps are involved in elucidating the mechanism of chemical growth:

1) Profile measurements of species concentrations for stable molecules and highly reactive radicals in a laminar, two-dimensional flame. Until recently, quantitative data on intermediate hydrocarbons and radicals in diffusion flames have not been available.

2) Determination of production and destruction rates of intermediate hydrocarbons from the analysis of species concentration data accompanied by temperature and velocity profile measurements. Since the early steps of hydrocarbon growth chemistry are rate-limiting, it is important to establish how rapidly species are formed and destroyed. This analysis is the two-dimensional analog (see below) of the recent comprehensive studies on premixed flames (*11, 13*).

3) Testing of proposed routes of chemical growth by comparing experimental values for net production and destruction rates based on flame measurements with estimated rates for specific elementary chemical growth steps. In this way possible paths for the formation of aromatic hydrocarbons can be evaluated.

Profile Measurements

Detailed species profiles have been recently measured in an atmospheric pressure methane/air diffusion flame with several optical techniques that provide relative concentrations as well as with quantitative mass spectrometric sampling methods (*18*). A Wolfhard-Parker burner that consists of a central fuel slot and two adjacent air slots (Fig. 1) is an attractive choice for these studies. A long path of uniform composition and temperature is accessible in the two-dimensional flame that is produced. Two flame sheets are formed at the fuel/air interfaces, and thus all species profiles are symmetric about the burner centerline. The analysis of transport processes in this two-dimensional flame system is a logical extension of the studies performed in one-dimensional premixed flames (*11, 13*).

Measurements of the temperature and velocity fields have also been performed. The temperature profiles were obtained with a fine wire (uncoated, 125 μm in diameter) Pt/Pt-10%Rh thermocouple. Corrections due to radiation effects were less than 7% at the highest temperatures in this flame (*18*); corrections due to catalytic effects are expected to be small (*22*) and have the opposite sign. For the profiles of the convective velocity, both the vertical and horizontal components were measured with laser Doppler velocimetry. Figure 2A illustrates the temperature and velocity fields for this flame. Many of the streamlines exhibit trajectories that originate in the lean region of the flame (on the air side of the flame sheets), cross the high-temperature primary reaction zones (the shaded regions that are 6.0 to 7.5 mm from the burner centerline), and continue into the fuel-rich regions.

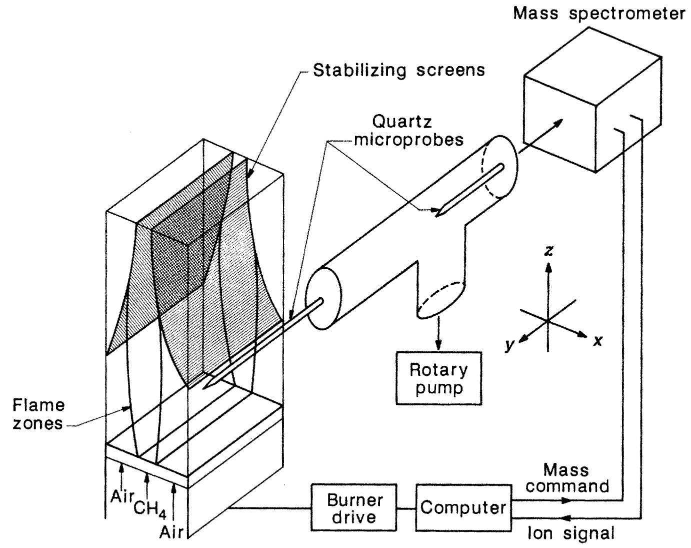

Fig. 1. Schematic diagram of the Wolfhard-Parker slot burner and the mass spectrometric sampling system (*18, 24*). The quartz microprobe is aligned parallel to the burner slots. For the optical studies (*18, 23*) the laser beam is also directed along the axis of the burner to take advantage of the two-dimensional flame geometry.

The optical measurements have included laser-induced fluorescence of OH and PAHs; multiphoton ionization of methyl radicals, nitric oxide, and small soot particles; photodissociation of large molecules to produce C_2 fragments; and Rayleigh scattering profiles (*18, 23*). Since only relative concentrations have been obtained, these results have provided a qualitative description of the chemical structure of the methane/air diffusion flame. The location of the primary reaction zones and peak concentrations of large molecules as well as the formation region for the earliest soot particles have been delineated.

In order to calculate production and destruction rates for specific molecules, quantitative concentration data are necessary. In this regard, the mass spectrometric measurements are of critical importance. Profiles of stable flame species have been collected with a direct-sampling mass spectrometer that was equipped with a quartz microprobe (orifice diameter ≈ 140 μm). Absolute concentrations of the major species (methane, oxygen, nitrogen, carbon dioxide, carbon monoxide, water, and hydrogen) and of acetylene, butadiene, and toluene were determined with a direct calibration procedure (*18*). Profiles of methylacetylene (or of allene, or both), vinylacetylene, diacetylene, triacetylene, benzene, and naphthalene were measured and calibrated indirectly. Ethylene concentrations were obtained by monitoring the mass 25 and 27 fragment ions at electron energies of 20 and 40 eV and making appropriate calibrations for acetylene and ethylene at these two ionization energies. Figure 2, B and C, illustrates the methane/air flame and presents the concentration contours for benzene, which is the first aromatic hydrocarbon species that is formed. Benzene is observed in spatially localized regions, and its concentration increases rapidly with increasing height H above the burner.

Successful profile measurements of methyl radicals have also been made with a quartz microprobe that was modified so that iodine vapor could be introduced inside the quartz tube (*24*). The sampled methyl radicals reacted quantitatively in the tip of the scavenger probe to form methyl iodide (*25*), which could then be detected in the mass spectrometer. These results represent an important check on possible disturbances caused by the quartz microprobe. Figure 3 compares the optical (*23*) and mass spectrometric (*24*) profiles of the methyl radical. Excellent agreement in the location and shape of the profiles is evident considering that the spatial resolution of the quartz microprobe [≈0.7 mm (*18*)] is larger than that of the multiphoton ionization experiments (≤0.1 mm).

Production and Destruction Rates

The role of specific elementary steps in proposed routes of chemical growth processes can be evaluated by determining how rapidly species are formed and destroyed. Since a laminar flame is a steady-state system, all species concentrations at any specific location are time-invariant. Thus convective and diffusive transport of material into and out of any given volume element must be exactly balanced by the chemical production and destruction processes. This can be expressed by

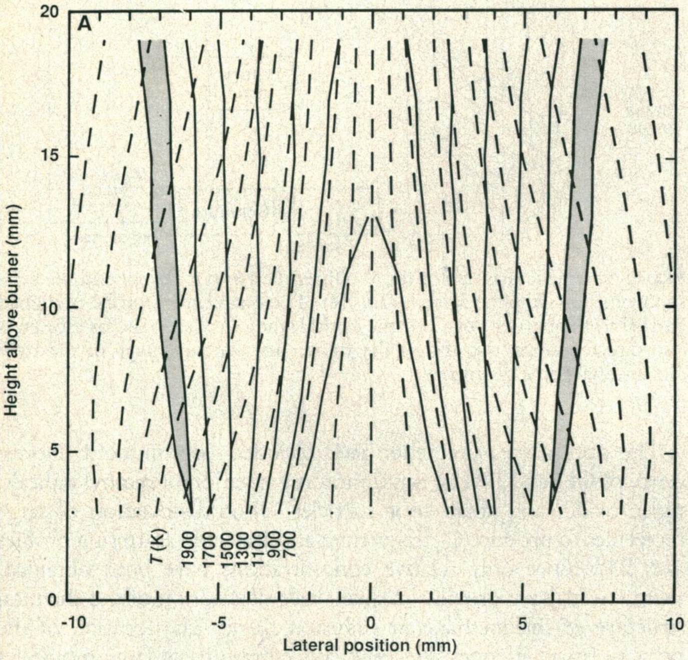

$$R_i = \nabla[N_i\ (v + V_i)] \tag{1}$$

where R_i is the net chemical rate, ∇ is the gradient operator (the derivative with respect to lateral position and height), N_i is the species concentration, v is the convective velocity, and V_i is the net diffusion velocity of the species into the local mixture. The diffusion velocity is given by (*26*):

$$V_i = -D_{i,\mathrm{mix}}[\nabla \ln(x_i) + (k_T/x_i)\nabla \ln(T)] \tag{2}$$

where x_i is the mole fraction of species i, $D_{i,\mathrm{mix}}$ is the diffusion coefficient for species i into the local mixture, and k_T is the thermal diffusion ratio. Values for $D_{i,\mathrm{mix}}$ have been determined from the contributions of all the major species and are given by:

$$D_{i,\mathrm{mix}} = (1 - x_i)/[\sum_j (x_j/D_{ij})] \tag{3}$$

where the sum is taken over j ≠ i and where the D_{ij} are the binary diffusion coefficients that were calculated by the method of Fristrom and Westenberg (*26*). In addition, the contributions from thermal diffusion have been estimated by calculating values for binary mixtures. For intermediate hydrocarbons the flux due to thermal diffusion is small compared to the convection and concentration-driven diffusion terms (*27*) and therefore makes no significant contribution to the results discussed below.

Rates of chemical production have been computed by numerical

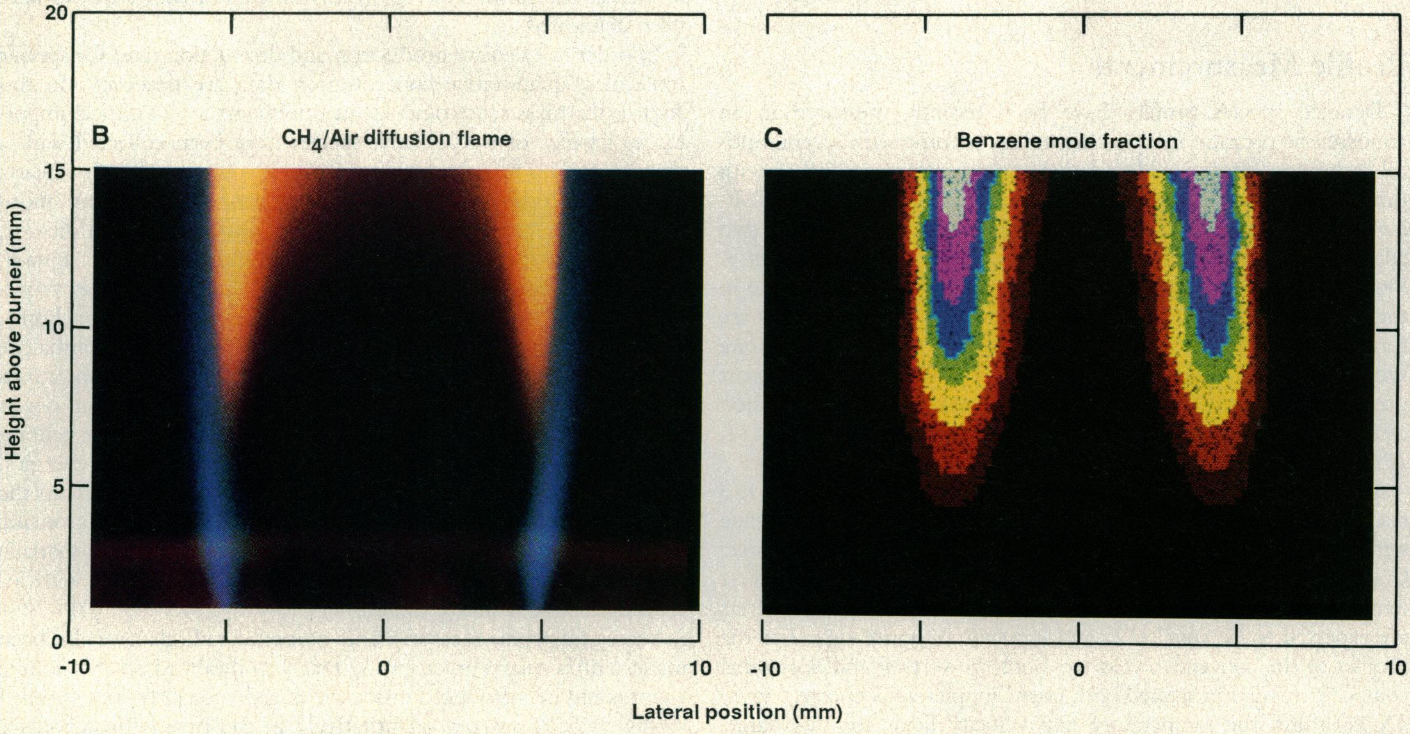

Fig. 2. (**A**) Isothermal contours (solid lines, temperature T in kelvin) determined from thermocouple measurements and streamlines (dashed lines) calculated from velocity measurements in a methane/air diffusion flame (*18*). The shaded areas denote the high-temperature primary reaction zones. (**B**) The lower portion of the methane/air diffusion flame. The blue emission is a result of CO oxidation in the high-temperature primary reaction zones, and the yellow luminosity arises from incandescent soot particles. (**C**) Benzene concentration contours. The benzene concentration increases with height above the burner; the maximum concentration (shown as white) extends over a mole fraction range from 4.9×10^{-4} to 5.6×10^{-4}, and the minimum concentration contour extends over a mole fraction range from 0.98×10^{-4} to 1.6×10^{-4}.

differentiation of Eq. 1 by using profile data at a particular height H as well as data from heights $H \pm 2$ mm. Figure 4 shows the calculated net chemical rates of production and destruction for acetylene for $H = 9$ mm and also includes the contributions from convection and concentration-driven diffusion. Acetylene is the most abundant product of hydrocarbon pyrolysis reactions and thus is an important growth species in proposed routes of soot formation. It can be seen that convection transports material across the high-temperature primary reaction zone toward the burner centerline (see Fig. 2A). In contrast, diffusion away from the burner centerline leads to the destruction of acetylene by bringing it into the high-temperature oxidation region of the flame.

By following the rates of production and destruction for acetylene as a function of H, a new feature is observed at higher flame positions (Fig. 5). At low positions in the flame the largest destruction rate ($R_i = -1.8 \times 10^{-5}$ mol cm^{-3} sec^{-1}) occurs near the high-temperature primary reaction zone. The production rate feature ($R_i = 3.2 \times 10^{-5}$ mol cm^{-3} sec^{-1}) occurs slightly toward the fuel-rich side. However, for $H \geq 13$ mm, the production rate peak is significantly diminished by a new destruction feature (see arrow in Fig. 5).

The acetylene destruction feature observed at higher flame positions is attributed to surface growth chemistry on small soot particles. This conclusion is based on premixed flame studies and optical detection of the earliest soot particles in diffusion flames. Harris and Weiner have performed measurements and an analysis which identify acetylene as the primary molecule responsible for soot particle growth in fuel-rich, premixed flames (*2–4*). The surface area available for growth of incipient soot particles per unit volume element in the flame had a measured value of ≈ 1.0 cm^2 cm^{-3}, and a specific surface growth rate of $\approx 8 \times 10^{-5}$ g cm^{-2} sec^{-1} was determined in ethylene flames (*2, 3*). Similar values have also been reported for methane/oxygen premixed flames (*28*) and for ethylene and propane diffusion flames (*29*). If we assume that the incipient soot particles in the methane/air diffusion flame exhibit surface areas and specific surface growth rates that are similar to those found in fuel-rich premixed flames and in diffusion flames of other fuels, then the magnitude of the change in total soot mass can be estimated to be 8×10^{-5} g cm^{-3} sec^{-1}, which is equivalent to an acetylene destruction rate of 3×10^{-6} mol cm^{-3} sec^{-1}. This value agrees quantitatively with the magnitude of the destruction feature shown in Fig. 5 for $H = 13$ mm. Furthermore, in the experiments on the

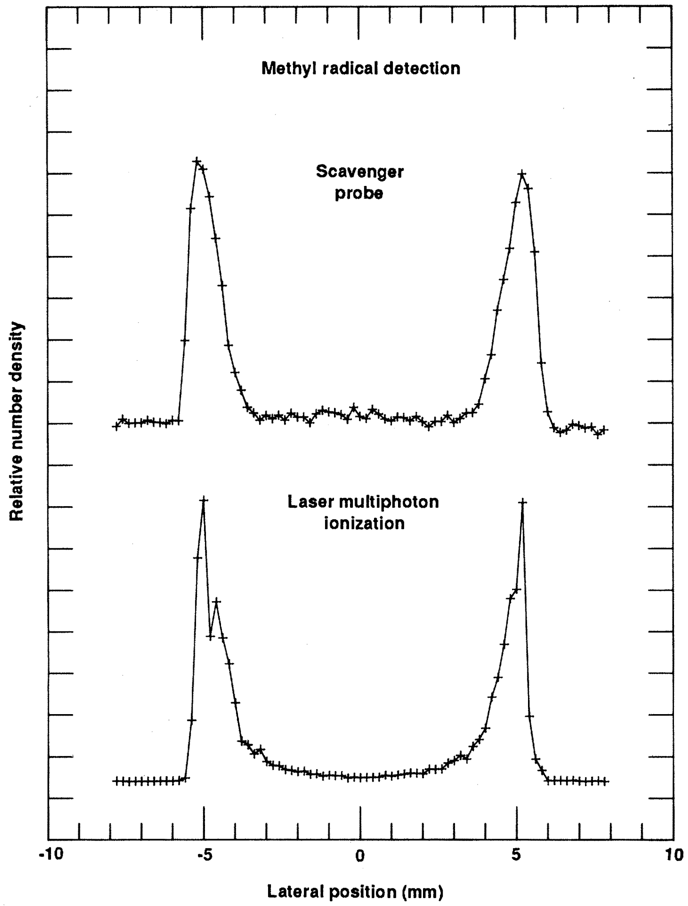

Fig. 3. Comparison of methyl radical profiles obtained by mass spectrometric scavenger probe sampling at a height H of 3.2 mm above the burner [top (*24*)] and by laser multiphoton ionization at $H = 3.0$ mm [bottom (*23*)]. The spatial resolution of the quartz microprobe is ≈ 0.7 mm, whereas that of the multiphoton ionization experiments is ≤ 0.1 mm (*18, 23*).

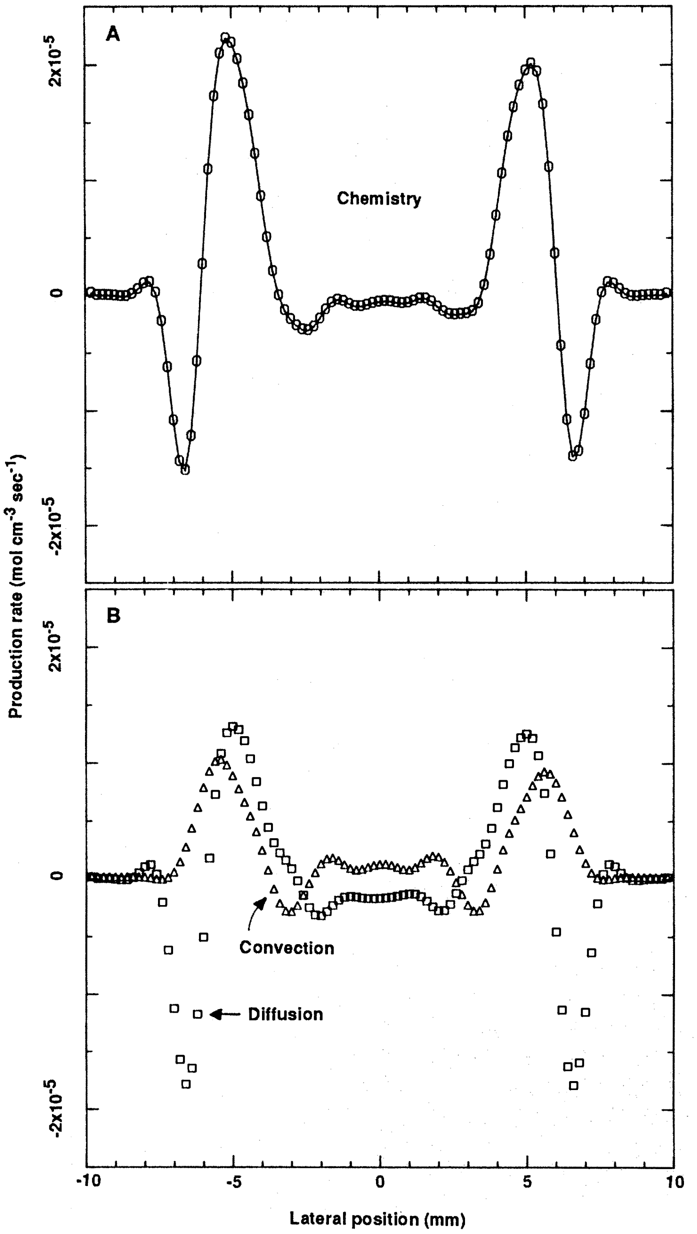

Fig. 4. Contributions to the rates of production and destruction of acetylene in a methane/air diffusion flame for $H = 9$ mm. (**A**) Net chemical rate of production and destruction; (**B**) concentration-driven diffusion (□) and convection (△) rates. The contribution due to thermal diffusion is negligible (*27*).

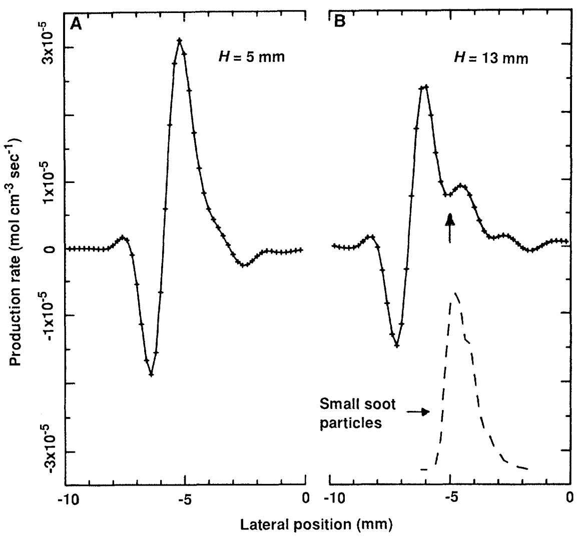

Fig. 5. Profiles of the net chemical rate of production and destruction for acetylene at *H* equal to (**A**) 5 mm and (**B**) 13 mm in a methane/air diffusion flame (solid lines; only the left-hand side is shown). The arrow denotes the new destruction feature which appears at higher flame positions. Also illustrated in (B) is the profile of small soot particles that was obtained by a laser ionization method at *H* = 12 mm [dashed line (*18*)].

methane/air diffusion flame the location of the decrease in the acetylene production rate profile lies close to the peak concentrations of small soot particles detected in profile measurements (*18*) (see Fig. 5). Surface growth occurs near the position where the particles are observed since particle diffusion is negligible. Thus this observation supports the attribution of the new loss process for acetylene to surface growth on the soot particles.

Similar behavior was also observed in the rates of production and destruction for diacetylene. In this case the new destruction feature which appears at higher flame positions represents a mass decrease of ≈5% compared to that found for acetylene. Harris and Weiner (*4, 30*) have estimated that diacetylene contributes approximately 10 to 15% of the mass added by surface growth in rich premixed flames and that the balance arises from acetylene addition reactions. Thus their observations on surface growth processes correspond closely with the methane/air diffusion flame measurements.

The results in premixed and diffusion flames described above suggest that the surface chemistry of particle growth is independent of flame environment. Is it also true that the chemical steps of molecular growth are independent of combustion conditions?

Testing Routes for Chemical Growth

The chemical steps of molecular growth from small hydrocarbon molecules to aromatic species and eventually to soot particles are not well established for flame conditions. From several studies performed in shock tubes (*31–33*) and in premixed flames (*11, 13*), specific mechanisms have been proposed and predictions have been compared to measured species concentration profiles. Available kinetic models successfully reproduce the experimental results for the major species but serious discrepancies arise for radicals and intermediate hydrocarbons (*15, 16*). The recent reaction path analysis of Westmoreland *et al.* (*16*), in which reaction rates for a given predicted profile are compared so that the dominant production and destruction reactions can be identified, is an important step in evaluating a particular mechanism.

With detailed species profile measurements and the determination of production and destruction rates of intermediate hydrocarbons, new data are now available to test proposed reaction mechanisms derived from shock tube and premixed flame studies. Since acetylene is an abundant product of hydrocarbon pyrolysis, the radicals produced by the addition of hydrogen atoms to acetylene and by the abstraction from acetylene [vinyl ($C_2H_3\cdot$) and ethynyl ($C_2H\cdot$), respectively] have often been postulated as important intermediates in chemical growth. For example, in the following mechanism (*13, 32–34*), the vinyl radical is the key species in the formation of benzene (C_6H_6):

$$H\cdot + C_2H_2 + M \rightleftarrows C_2H_3\cdot + M \tag{A1}$$

$$H\cdot + C_2H_4 \rightleftarrows C_2H_3\cdot + H_2 \tag{A1'}$$

$$C_2H_3\cdot + C_2H_2 \rightleftarrows C_4H_5\cdot \tag{A2}$$

$$C_4H_5\cdot \rightleftarrows C_4H_4 + H\cdot \tag{A3}$$

$$C_4H_4 + C_2H_3\cdot \rightleftarrows C_6H_7\cdot \tag{A4}$$

$$C_4H_5\cdot + C_2H_2 \rightleftarrows C_6H_7\cdot \tag{A4'}$$

$$C_6H_7\cdot \rightleftarrows \text{cyclic } C_6H_7\cdot \tag{A5}$$

$$\text{Cyclic } C_6H_7\cdot \rightleftarrows C_6H_6 + H\cdot \tag{A6}$$

where M is a third-body molecule. Alternatively, some workers have proposed that the ethynyl radical is important, particularly at higher temperatures (*31, 33*):

$$H\cdot + C_2H_2 \rightleftarrows C_2H\cdot + H_2 \tag{B1}$$

$$C_2H\cdot + C_2H_2 \rightleftarrows C_4H_3\cdot \tag{B2}$$

$$C_2H_2 + C_4H_3\cdot \rightleftarrows \text{linear } C_6H_5\cdot \tag{B3}$$

$$\text{Linear } C_6H_5\cdot \rightleftarrows \text{cyclic } C_6H_5\cdot \text{ (phenyl radical)} \tag{B4}$$

$$\text{Cyclic } C_6H_5\cdot + H\cdot + M \rightleftarrows C_6H_6 + M \tag{B5}$$

A viable mechanism must account not only for the observed steady-state concentrations of the species involved in chemical

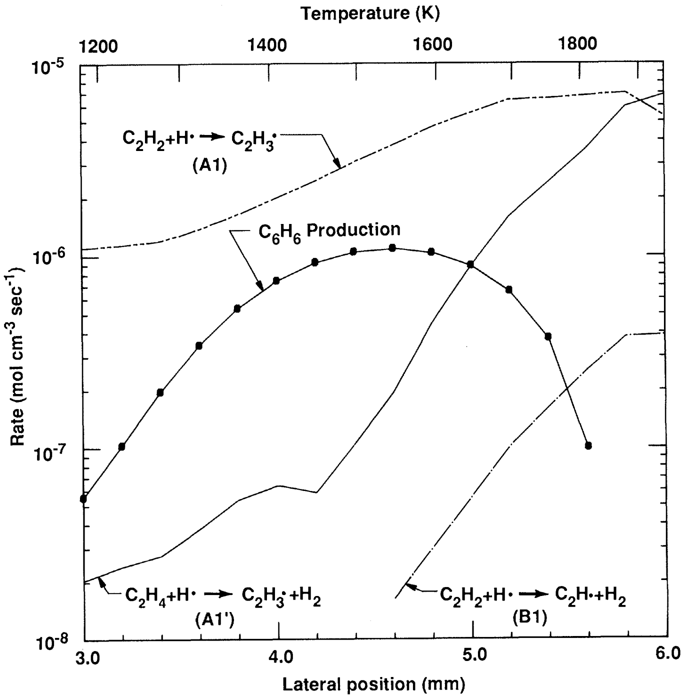

Fig. 6. Comparison of the net chemical production rate of benzene measured in a methane/air diffusion flame (shown as the points) with the maximum production rates estimated for vinyl radicals (reactions A1 and A1′) and ethynyl radicals (reaction B1) at *H* = 9 mm. Only the data for the right-hand side of the flame are presented. Also shown at the top of the figure are the thermocouple temperature measurements, which have been corrected for radiation losses (*18*).

growth processes but also for the chemical fluxes of these intermediates. Specifically, one can compare the predictions of mechanisms A and B for the production rates of the vinyl and ethynyl radicals in the forward direction with the observed net production rate of benzene. For a given chemical pathway to be feasible, the production rate of these initial radical species must be at least as great as the measured net chemical production rate for any subsequent product molecule as determined from the experimental flame data.

Comparison of production rates of intermediate species with the formation of the first aromatic ring is a convenient starting point for evaluating a proposed mechanism for chemical growth reactions. The required profile data are now available for the small, stable hydrocarbons, and reasonable estimates for the needed radical concentrations can be obtained (see below). Quantitative concentration measurements for larger stable hydrocarbons (such as naphthalene) and larger radicals (such as $C_4H_n\cdot$) have not yet been made. The formation of benzene itself may or may not be essential to soot production, although modeling of both shock tube and premixed flame results indicates that this is a key rate-limiting step (*32, 34*). Mechanisms of chemical growth that bypass the formation of a C_6H_n aromatic ring compound (*35*) could also be analyzed.

The production rates of vinyl and ethynyl radicals can be calculated if we know the concentration profile of hydrogen atoms (see reactions A1, A1′, and B1), which can be determined from the measured profiles of hydrogen, methane, and the methyl radical if the process

$$CH_4 + H\cdot \rightleftarrows CH_3\cdot + H_2 \qquad (4)$$

is fully equilibrated. By using measured species concentration data and rate constants from the literature (*36*), the reaction rates were found to be much faster in both the forward and the reverse directions than the transport processes of diffusion and convection. Thus reasonably accurate hydrogen atom concentrations may be obtained.

Figure 6 shows the comparison of the observed net production rate for benzene with the forward production rates of the vinyl radical (through reactions A1 and A1′) and the ethynyl radical (through reaction B1) for $H = 9$ mm. This height was chosen for the analysis because the concentrations of aromatic species are appreciable and the acetylene concentration has not yet been diminished by surface growth addition processes on particles. Note that the results for the production rates span a temperature range from 1150 to 1900 K. The production rate of the vinyl radical produced in reaction A1 exceeds the net benzene production rate throughout the flame region where benzene is formed. Reaction A1′ also contributes significantly at high temperatures. In contrast to vinyl radical production, the ethynyl radical formation rate in reaction B1 is always less than the maximum net production rate for benzene. For reactions A1 and A1′ the forward rates are much faster than the reverse rates, and therefore equilibrium favors the formation of the vinyl radical. However, the equilibrium of reaction B1 favors C_2H_2 and $H\cdot$ relative to $C_2H\cdot$ and H_2, and thus the net rate of ethynyl radical formation is actually much less than that shown in Fig. 6 and cannot account for the observed formation of benzene. These results indicate that the vinyl radical can be a key intermediate in chemical growth reactions which lead to aromatic ring formation and that the ethynyl radical produced by reaction B1 is not important. Another possible route for ethynyl radical production is

$$OH\cdot + C_2H_2 \rightleftarrows C_2H\cdot + H_2O \qquad (B1')$$

Quantitative $OH\cdot$ concentrations would be required to assess the importance of this process. If the $OH\cdot$ concentration is as large as 10^{-4} mole fraction at a lateral position of 6 mm, then the production of $C_2H\cdot$ by reaction B1′ in the forward direction is estimated to be fast enough to account for the measured net benzene production.

Conclusions and Outlook

Research on the methane/air diffusion flame described in this article has led to several significant results. Species profile measurements in the soot inception region have identified which species are present, where they are located, and their concentrations. Analysis of these data to give production and destruction rates for intermediate hydrocarbons has yielded the first evidence in diffusion flames for the important role of acetylene in surface growth reactions. In addition, new tests of proposed chemical growth mechanisms implicate the vinyl radical as an important key precursor species.

The analysis described above has concentrated on comparing maximum production rates for vinyl and ethynyl radicals with the net formation rate of benzene. In order to establish that a particular mechanism for benzene formation is viable, it is necessary to examine each elementary step and to include the production rates for the C_3H_n and C_4H_n hydrocarbons. This is straightforward for stable molecules but is difficult for radicals. Reactions analogous to reaction 4 are often not equilibrated (that is, the chemical reactions are not much faster than the transport processes), and direct measurements of these radical concentrations are not available in diffusion flames.

Of broader significance will be attempts to address questions that concern the effects of different hydrocarbon fuels on the pathways that lead to soot formation. Can the conclusion that the vinyl radical is a key species for chemical growth be generalized? Initial measurements in diffusion flames show a wide variation in the peak concentrations of intermediate hydrocarbons as the fuel is changed (*20*). There is a need to determine species fluxes and to identify the important radical intermediates for different hydrocarbon fuels, including aromatic compounds.

Finally, how does the analysis of diffusion flame measurements compare with the results from premixed flames? This issue is of special significance since premixed flame data on species concentrations (*11, 13*) are more comprehensive than the diffusion flame measurements, particularly for radicals. If the dominant routes for chemical growth are the same for premixed and diffusion flames, then the results from the extensive analyses and modeling investigations of the former can be used to unravel the interactions between chemical and transport processes in the latter. Some intriguing similarities have recently emerged.

1) Acetylene is the major growth species in the region of particle inception for both premixed and diffusion flames (*2–4, 27*). In addition, the surface reactivity for young soot particles is essentially the same in both environments (*2, 3, 29*). This important role of acetylene in surface growth has been expected (*2, 37*). Nevertheless, it is interesting that the surface growth chemistry seems to be independent of flame environment and hydrocarbon fuel.

2) Results in the methane/air diffusion flame indicate that the process of polyacetylenic growth

$$C_2H\cdot + C_2H_2 \rightleftarrows C_4H_2 + H\cdot$$
$$C_4H_2 + C_2H\cdot \rightleftarrows C_6H_2 + H\cdot$$
$$C_6H_2 + C_2H\cdot \rightleftarrows C_8H_2 + H\cdot$$

represents a parallel growth pathway that is not involved in the formation of aromatic compounds (*27*). Similarly, Harris *et al.* (*38*) found that diacetylene is not kinetically coupled with species that participate in other hydrocarbon growth processes.

3) The maximum net production rate for benzene formation is identical in the methane/air diffusion flame (Fig. 6) and in a fuel-rich, premixed butadiene/oxygen/argon flame studied by Cole *et al.* [figure 10 in (*13*)].

Thus far the results from diffusion flames reveal striking parallels with the results for premixed flames. It is tempting to conclude that a single dominant mechanism is involved in hydrocarbon growth chemistry for all flaming combustion conditions.

REFERENCES AND NOTES

1. K. P. Schug, Y. Manheimer-Timnat, P. Yaccarino, I. Glassman, *Combust. Sci. Technol.* **22**, 235 (1980); I. Glassman and P. Yaccarino, in *Eighteenth Symposium (International) on Combustion* (The Combustion Institute, Pittsburgh, 1981), p. 1175; A. Gomez, G. Sidebotham, I. Glassman, *Combust. Flame* **58**, 45 (1984).
2. S. J. Harris and A. M. Weiner, *Combust. Sci. Technol.* **31**, 155 (1983).
3. ———, *ibid.* **32**, 267 (1983).
4. ———, *ibid.* **38**, 75 (1984).
5. J. H. Kent and H. Gg. Wagner, *ibid.* **41**, 245 (1984); R. J. Santoro and H. G. Semerjian, in *Twentieth Symposium (International) on Combustion* (The Combustion Institute, Pittsburgh, 1985), p. 997.
6. H. F. Calcote, *Combust. Flame* **42**, 215 (1981).
7. B. D. Crittenden and R. Long, *ibid.* **20**, 359 (1973).
8. K. H. Homann and H. Gg. Wagner, in *Eleventh Symposium (International) on Combustion* (The Combustion Institute, Pittsburgh, 1967), p. 371.
9. S. W. Benson, in *Nineteenth Symposium (International) on Combustion* (The Combustion Institute, Pittsburgh, 1982), p. 1350; M. Weissman and S. W. Benson, *Int. J. Chem. Kinet.* **16**, 307 (1984).
10. K. H. Homann and H. Gg. Wagner, *Ber. Bunsenges. Phys. Chem.* **69**, 20 (1965); U. Bonne, K. H. Homann, H. Gg. Wagner, in *Tenth Symposium (International) on Combustion* (The Combustion Institute, Pittsburgh, 1965), p. 503; J. C. Biordi, *Prog. Energy Combust. Sci.* **3**, 151 (1977) and references therein.
11. J. D. Bittner and J. B. Howard, in *Eighteenth Symposium (International) on Combustion* (The Combustion Institute, Pittsburgh, 1981), p. 1105; in *Particulate Carbon: Formation During Combustion*, D. C. Siegla and G. W. Smith, Eds. (Plenum, New York, 1981), p. 109; J. B. Howard and J. D. Bittner, in *Soot in Combustion Systems and Its Toxic Properties*, J. Lahaye and G. Prado, Eds. (Plenum, New York, 1983), p. 57; J. D. Bittner, J. B. Howard, H. B. Palmer, *ibid.*, p. 95; J. D. Bittner, thesis, Massachusetts Institute of Technology (1981); ——— and J. B. Howard, in *Nineteenth Symposium (International) on Combustion* (The Combustion Institute, Pittsburgh, 1982), p. 211.
12. J. Warnatz, H. Bockhorn, A. Möser, H. W. Wenz, in *Nineteenth Symposium (International) on Combustion* (The Combustion Institute, Pittsburgh, 1982), p. 197; H. Bockhorn, F. Fetting, H. W. Wenz, *Ber. Bunsenges. Phys. Chem.* **87**, 1067 (1983); E. W. Kaiser, W. G. Rothschild, G. A. Lavoie, *Combust. Sci. Technol.* **33**, 123 (1983); *ibid.* **41**, 271 (1984).
13. J. A. Cole, J. D. Bittner, J. P. Longwell, J. B. Howard, *Combust. Flame* **56**, 51 (1984).
14. J.-L. Delfau and Ch. Vovelle, *J. Chim. Phys.* **82**, 747 (1985); W. G. Rothschild, E. W. Kaiser, G. A. Lavoie, *Combust. Sci. Technol.* **47**, 209 (1986).
15. R. J. Hennessy, C. Robinson, D. B. Smith, in *Twenty-First Symposium (International) on Combustion* (The Combustion Institute, Pittsburgh, 1987), in press.
16. P. R. Westmoreland, J. B. Howard, J. P. Longwell, *ibid.*
17. S. R. Smith and A. S. Gordon, *J. Phys. Chem.* **60**, 759 (1956); A. S. Gordon, S. R. Smith, J. R. McNesby, in *Seventh Symposium (International) on Combustion* (The Combustion Institute, Butterworths, London, 1959), p. 317; P. Dearden and R. Long, *J. Appl. Chem. (London)* **18**, 243 (1968); H. Tsuji and I. Yamaoka, in *Twelfth Symposium (International) on Combustion* (The Combustion Institute, Pittsburgh, 1969), p. 997; G. Spengler and J. Kern, *Brennst. Chem.* **50**, 321 (1969); J. Kern and G. Spengler, *Erdöl Kohle Erdgas Petrochem.* **23**, 813 (1970); H. Tsuji and I. Yamaoka, in *Thirteenth Symposium (International) on Combustion* (The Combustion Institute, Pittsburgh, 1971), p. 723; J. W. Aldred, J. C. Patel, A. Williams, *Combust. Flame* **17**, 139 (1971); S. R. Gollahalli and T. A. Brzustowski, in *Fourteenth Symposium (International) on Combustion* (The Combustion Institute, Pittsburgh, 1973), p. 1333; J. H. Kent and F. A. Williams, in *Fifteenth Symposium (International) on Combustion* (The Combustion Institute, Pittsburgh, 1975), p. 315; S. I. Abdel-Khalik, T. Tamaru, M. M. El-Wakil, *ibid.*, p. 389; G. P. Prado, M. L. Lee, R. A. Hites, D. P. Hoult, J. B. Howard, in *Sixteenth Symposium (International) on Combustion* (The Combustion Institute, Pittsburgh, 1977), p. 649; I. Yamaoka and H. Tsuji, *ibid.*, p. 1145; R. E. Mitchell, A. F. Sarofim, L. A. Clomburg, *Combust. Flame* **37**, 201 (1980); *ibid.*, p. 227.
18. K. C. Smyth, J. H. Miller, R. C. Dorfman, W. G. Mallard, R. J. Santoro, *Combust. Flame* **62**, 157 (1985).
19. K. Saito, F. A. Williams, A. S. Gordon, *J. Heat Transfer* **108**, 640 (1986).
20. A. Hamins, A. S. Gordon, K. Seshadri, K. Saito, in *Twenty-First Symposium (International) on Combustion* (The Combustion Institute, Pittsburgh, 1987), in press; W. Bartok and R. J. Kuriskin, poster paper 3 presented at the Twenty-First Symposium (International) on Combustion (The Combustion Institute), Munich, West Germany, August 1986.
21. C. Vovelle, J.-L. Delfau, M. Reuillon, E. Bastin, D. Poutiers, poster paper 112 presented at the Twenty-First Symposium (International) on Combustion (The Combustion Institute), Munich, West Germany, August 1986.
22. S. M. Schoenung and R. K. Hanson, *Combust. Sci. Technol.* **24**, 227 (1981).
23. K. C. Smyth and P. H. Taylor, *Chem. Phys. Lett.* **122**, 518 (1985).
24. J. H. Miller and P. H. Taylor, *Combust. Sci. Technol.*, in press.
25. R. M. Fristrom, *Science* **140**, 297 (1963); in *Ninth Symposium (International) on Combustion* (The Combustion Institute, Academic Press, New York, 1963), p. 560; *Combust. Flame* **50**, 239 (1983).
26. ——— and A. A. Westenberg, *Flame Structure* (McGraw-Hill, New York, 1965), chap. 5.
27. J. H. Miller, W. G. Mallard, K. C. Smyth, in *Twenty-First Symposium (International) on Combustion* (The Combustion Institute, Pittsburgh, 1987), in press.
28. E. R. Ramer, J. F. Merklin, C. M. Sorensen, T. W. Taylor, *Combust. Sci. Technol.* **48**, 241 (1986).
29. J. H. Kent and H. Gg. Wagner, *Combust. Flame* **47**, 53 (1982), analyzed in reference (*3*); U. Vandsburger, I. Kennedy, I. Glassman, *Combust. Sci. Technol.* **39**, 263 (1984); W. L. Flower and C. T. Bowman, paper 16 presented at *Chemical and Physical Processes in Combustion* (Eastern Section of The Combustion Institute, Philadelphia, PA, November 1985); H. S. Hura and I. Glassman, paper 50, *ibid.*
30. S. J. Harris and A. M. Weiner, *Annu. Rev. Phys. Chem.* **36**, 31 (1985).
31. T. Tanzawa and W. C. Gardiner, Jr., *J. Phys. Chem.* **84**, 236 (1980).
32. M. Frenklach, D. W. Clary, W. C. Gardiner, Jr., S. E. Stein, in *Twentieth Symposium (International) on Combustion* (The Combustion Institute, Pittsburgh, 1985), p. 887.
33. M. B. Colket III, in *Twenty-First Symposium (International) on Combustion* (The Combustion Institute, Pittsburgh, 1987), in press.
34. M. Frenklach and J. Warnatz, *Combust. Sci. Technol.*, in press.
35. A. B. Callear and G. B. Smith, *J. Phys. Chem.* **90**, 3229 (1986).
36. W. Tsang and R. F. Hampson, *J. Phys. Chem. Ref. Data* **15**, 1087 (1986).
37. J. H. Miller, K. C. Smyth, W. G. Mallard, in *Twentieth Symposium (International) on Combustion* (The Combustion Institute, Pittsburgh, 1985), p. 1139; see response to question by J. B. Howard.
38. S. J. Harris, A. M. Weiner, R. J. Blint, J. E. M. Goldsmith, in *Twenty-First Symposium (International) on Combustion* (The Combustion Institute, Pittsburgh, 1987), in press.

39. We are pleased to acknowledge the valuable contributions of W. G. Mallard, R. J. Santoro, R. C. Dorfman, P. H. Taylor, and T. A. Kohout to the diffusion flame measurements.